Commissioning and Validation of CT Number to SPR Calibration in Carbon Ion Therapy Facility

Yuya Miyasaka (PhD)[1,*], Takayuki Kanai (PhD)[2], Hikaru Souda (PhD)[1], Yoshifumi Yamazawa (MS)[3], Sung Hyun Lee (PhD)[1], Hongbo Chai (PhD)[1], Hiraku Sato (MD, PhD)[4], Takeo Iwai (PhD)[1]

[1] Department of Heavy Particle Medical Science, Yamagata University Graduate School of Medical Science, Yamagata, Japan
[2] Department of Radiation Oncology, Tokyo Women's Medical University, Shinjuku, Tokyo, Japan
[3] Department of Radiology, Yamagata University Hospital, Yamagata, Japan
[4] Department of Radiology, Yamagata University Faculty of Medicine, Yamagata, Japan

ARTICLE INFO

ABSTRACT

Purpose: We performed computed tomography (CT)—stopping power ratio (SPR) calibration in a carbon-ion therapy facility and evaluated SPR estimation accuracy.

Materials and Methods: A polybinary tissue model method was used for the calibration of CT numbers and SPR. As a verification by dose calculation, we created a virtual phantom to which the CT-SPR calibration table was applied. Then, SPR was calculated from the change in the range of the treatment planning beam when changing to 19 different CT numbers, and the accuracy of the treatment planning system (TPS) calculation of SPR values from the CT-SPR calibration table was validated. As a verification by measurement, 5 materials (water, milk, olive oil, ethanol, 40% K_2HPO_4) were placed in a container, and the SPR was obtained by measurement from the change in the range of the beam that passed through the materials.

Results: The results of the dose calculations of the TPS showed that the results agreed within 1% for the lower CT numbers up to 1000 HU, but there was a difference of 3.0% in the higher CT number volume. The difference between the SPR calculated by TPS and the SPR caused by the difference in the energy of the incident particles agreed within 0.51%. The accuracy of SPR estimation was measured, and the error was within 2% for all materials tested.

Conclusion: These results indicate that the SPR estimation errors are within the range of errors that can be expected in particle therapy. From commissioning and verification results, the CT-SPR calibration table obtained during this commissioning process is clinically applicable.

Introduction

For high-precision radiation therapy, it is essential to take into account the heterogeneity within the body in dose calculation. For this purpose, performing calibration of the computed tomography (CT) numbers and effective density using CT images is necessary.[1,2] In dose calculation for X-ray treatment planning, the effective density can be well approximated by the electron density, and commercially available phantoms and standardized methods are available.[3] In contrast, for particle therapy, it is necessary to determine the stopping power values of various tissues in beam paths. Currently, the most common method is

to register a calibration table that relates CT numbers to the stopping power ratio (SPR) to water in the treatment planning system.[4–7] Schneider et al pointed out that the materials used in commercial phantoms are not sufficiently equivalent to body tissues and proposed a stoichiometric calibration method to solve this problem.[8] This method applies an X-ray attenuation model determined from CT images to standard human body composition data and to the CT numbers and stopping power. Kanematsu et al proposed a simple and standardized method of calibrating the CT numbers and stopping power using the polybinary calibration method based on stoichiometric calibration, and this method is used at several facilities in Japan.[9,10]

Our facility started carbon-ion radiotherapy in 2021. Because the commissioning error of the calibration of CT values to SPRs has a significant impact on treatment, commissioning of this item should be performed extremely carefully. There have been several reports on commissioning and QA for CT-SPR,[11–14] as well as beam accuracy[15–17] and respiratory gating irradiation[18–20] as commissioning items for particle therapy facilities. For example, Peter et al analyzed multicenter data on CT-SPR conversion tables for proton therapy facilities in Europe and published their data as a consensus.[11] Similarly, it is important to analyze and publish the findings of the CT-SPR conversion method in carbon-ion treatment facilities, which are expected to increase in the future.

Therefore, herein, we report on a method of commissioning and evaluation of CT-SPR calibration in a carbon-ion beam therapy facility.

Material and methods

CT-SPR calibration method

The CT-SPR calibration method was based on the polybinary tissue model reported by Kanematsu et al.[10] This method approximates the human body tissue as polybinary mixture of muscle, air, fat, and bone and uses the stoichiometric method to obtain conversion relations from the CT numbers of 4 samples of water, air, 100% ethanol, and a 40% K_2HPO_4 solution as materials for each component. This method is an updated version[10] of the previous method[9] and has been used in several particle therapy facilities in Japan.

CT scan protocol

In this study, we used a 320-multidetector CT scanner (Aquilion ONE Canon Medical Systems, Otawara, Japan). The scan protocols for clinical use in our facility are shown in Table 1. The Head and Neck Helical protocol is used for head and neck treatment, the Body Volume protocol is used if 4-dimensional CT is necessary for the treatment of moving targets, and the Body Helical protocol is applied for the other treatment.

CT-SPR calibration phantoms and data acquisition

For CT-SPR calibration, we used the same cylindrical type of phantom reported by Kusano et al that can be filled with water inside.[21,22] Two sizes of CT calibration phantom, large and small, were used for the phantom to acquire CT images of the material (Figure 1(a)). The phantom size diameters were Φ290 mm for the body and Φ190 mm for the head and neck. The inside of the phantom was filled with water, and there were places where the containers could be placed. The containers could be filled with arbitrary liquid materials, and their size was Φ20 mm in diameter and 200 mm in length. Each container was filled with water, air, 100% ethanol, and a 40% K_2HPO_4 solution. The 40% K_2HPO_4 solution was defined as a 40% aqueous solution by mass. We prepared 2 containers filled with of each sample and placed each material in 2 locations in the inner and peripheral parts of the phantom. The center of the installed phantom was placed to the origin of CT. The Phantom was scanned according to the CT imaging protocol conditions in Table 1. As an example, a CT image of a phantom

obtained with the Body Helical protocol is shown in Figure 1(b), and with Head and Neck protocol is shown in Figure 1(c). In the slice of the CT image origin, a region of interest (ROI) was placed in the center of each container. The ROI size was adjusted according to the diameter of the container. The mean CT numbers within the ROI were obtained for each material, and in addition, the mean CT numbers of the inner and peripheral containers were used as the CT numbers for each material. The obtained CT numbers were used to calculate the CT numbers of 11 different tissue substitutes according to the CT-SPR calibration method session.

Registration of CT-SPR calibration data to the treatment planning system

The carbon-ion radiotherapy planning system in our facility was the RayStation10A (RaySearch Laboratories, Stockholm, Sweden). We registered the CT numbers and the corresponding SPR values of the materials obtained by the calibration method reported by Kanematsu et al[10] into the RayStation. The registered reference energy was 131 MeV/u, which was proposed by Inaniwa et al as the effective kinetic energy of carbon ions.[23]

Verification by dose calculation

The virtual phantom was created to verify the accuracy of the CT-SPR calibration table in the dose calculation (Figure 2). The geometry of the virtual phantom consisted of a $15 \times 15 \times 33$ cm water volume (physical density, 1.00 g/cm^3) and $15 \times 15 \times 5$ cm volume with variable CT numbers, which was located upstream of the beam. A total of 19 patterns of the CT numbers (-2000, -1000, -800, -600, -400, -200, -150, -100, -50, 0, 50, 100, 200, 400, 1000, 2000, 3000, 4000, and 5000 HU) assigned alternatively to the variable CT number volume. The depth slice thickness of the phantom was 0.1 cm. A beam with an energy of 430 MeV/u was injected into the virtual phantom. The field size was 10×10 cm, and the spot spacing was 0.2 cm. A ridge filter was used in the spread-out Bragg peak formation. The ridge filter shaped the carbon beam so that 0.1 cm width at 1-sigma. The dose calculation grid size was set to 0.1 cm in the parallel direction of the beam and 0.4 cm in each axis in the perpendicular direction of the beam. The dose calculation algorithm was pencil beam.[24] We calculated the SPR used in dose calculation in the treatment planning system (SPR_{calc}) using the following equation:

$$SPR_{calc} = SPR_{0HU} \times \left(\frac{Range_{water} - Range_{xHU}}{5} \right) + 1 \qquad (1)$$

where SPR_{0HU} is the SPR at 0 HU in the CT-SPR calibration table, registered in the treatment planning system; $Range_{water}$ is the range of carbon-ion beam when water with a physical density of 1.00 g/cm^3 was assigned to the variable CT number volume; and $Range_{xHU}$ is the range when CT number of x HU was assigned to the variable CT number volume. The value 5 in the equation means that the thickness of the variable CT number volume is 5 cm, and SPR_{calc} was calculated from the difference in range per cm. The range was defined as the depth where the dose was 50% of the maximum dose after the Bragg peak. In this study, the SPR of water was considered to be 1, and the SPR was calculated from the difference in range relative to water. This is what is meant by $+1$ in the Equation (1). The difference between the SPR_{calc}

Table 1
CT scan protocol.

Protocol	Voltage (kV)	Tube current (mA)	FOV (mm)	Slice thickness (mm)	Interpolation	Reconstruction algorithm
Body helical	120	500	500	2	V-TCOT	FC13
Body volume	120	500	500	2	volume-Xact	FC13
Head and neck helical	120	500	500	2	V-TCOT	FC13

Abbreviations: CT, computed tomography; FOV, field of view.
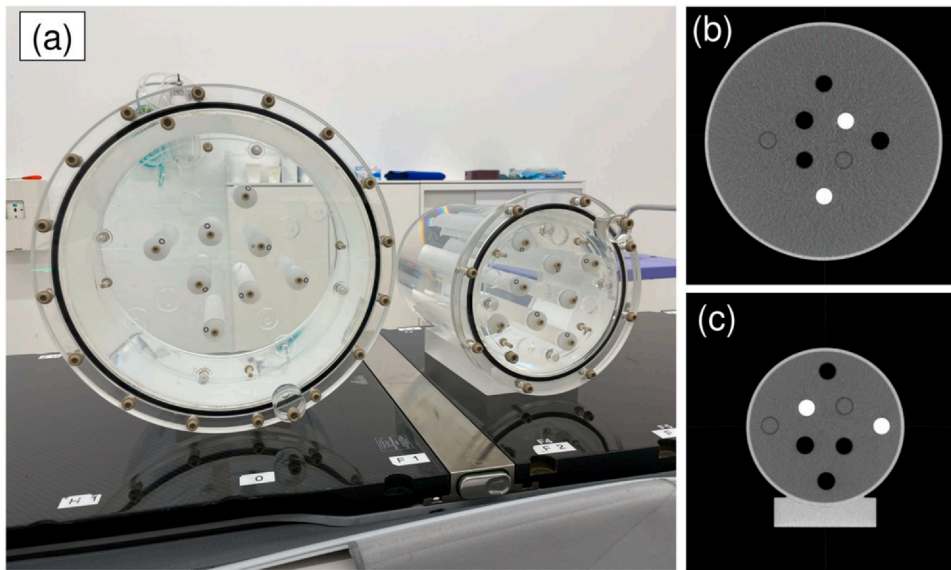
Figure 1. (a) shows an image of the phantom, with diameters of Φ290 cm and Φ190 cm, respectively. The interior is filled with water, and 4 containers are set up to hold tissue substitutes. (b) and (c) are CT images of a phantom of Φ290 cm and Φ190 cm in diameter, respectively. Four materials stored in containers were placed, one in the center of the phantom and one at each of the edges.

and $SPR_{register}$, which is the SPR corresponding to the CT numbers registered in the RayStation, was calculated using the following equation:

$$Diff_{calc.} \quad (\%) = \left(\frac{SPR_{calc} - SPR_{register}}{SPR_{register,water}} \right) \times 100 \tag{2}$$

The RayStation calculated the doses by taking into account the energy dependence of SPR. Therefore, there may be a difference between the $SPR_{register}$ and SPR_{calc} because the dose calculation was performed at 430 MeV/u, whereas the standard energy of the registered CT-SPR calibration table was 131 MeV/u. Hence, the possible errors calculated at different energies were verified. The theoretically expected difference in SPR ($Diff_{theoretical}$) between 131 and 430 MeV/u was calculated based on the Bethe–Bloch formula.[23] The SPR values were calculated for 11 core substances (water, air, lung, fat, muscle, cartilage, bone, bone+, aluminum, aluminum+, and iron) using the atomic compositions and physical densities listed in the RayStation reference manual.[25] $Diff_{theoretical}$ was calculated according to the following equation:

$$Diff_{theoretical}(\%) = \left(\frac{SPR_{430MeV/u} - SPR_{131MeV/u}}{SPR_{water}} \right) \times 100 \tag{3}$$

where $SPR_{430\,MeV}$ and $SPR_{131\,MeV}$ are the SPRs at 430 and 131 MeV/u calculated from the theoretical equations and SPR_{water} is the SPR of

water at 131 MeV/u calculated from the theoretical equations. $Diff_{calc.}$ and $Diff_{theoretical}$ were compared to test whether $Diff_{calc}$ is a theoretically explainable difference.

Verification by measurement

We verified the accuracy of CT-SPR calibration in the treatment planning system with measurements. Five easily available materials were used for validation: water, 100% ethanol, 40% K_2HPO_4 solution, commercial milk, and olive oil. First, the CT images of the 5 materials were acquired using the Body Helical protocol. Subsequently, the SPR of each material was estimated from the CT-SPR calibration table registered in the treatment planning system. For measurements, 5 materials were placed in containers in contact with the beam ports. The 430 MeV/u carbon-ion beams transmitted through the material was measured with a large-area parallel plane ion chamber with a diameter of 16 cm. The depth dose curves were measured at 0.1 mm intervals to determine the depth of the dose maximum point. A 3-dimensional water phantom (Toshiba Energy Systems, Kawasaki, Japan) was used as a measurement phantom. The $SPR_{meas,x}$ of the 5 materials x obtained by the measurement were calculated by using the following equation:
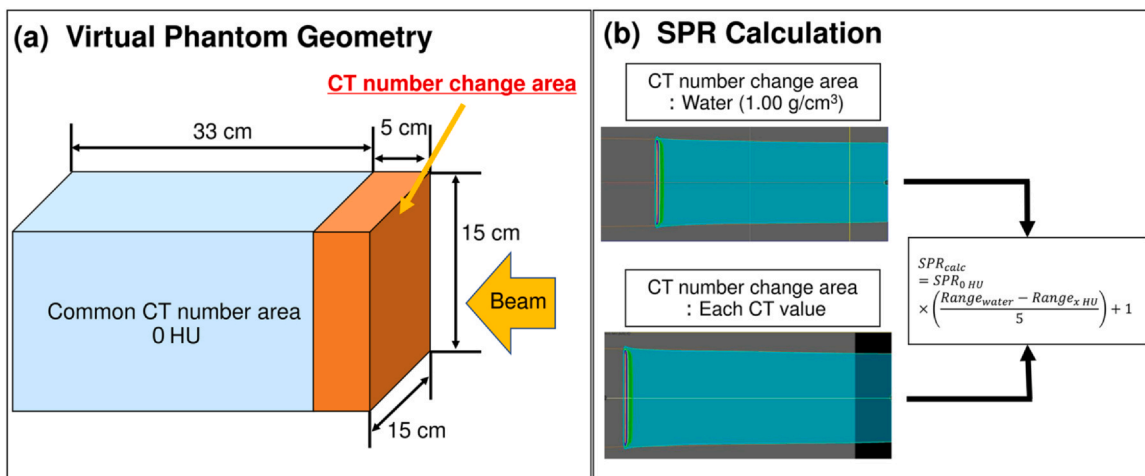
Figure 2. (a) shows the geometry of the virtual phantom created in the treatment planning system. A volume to change the CT number is set upstream of the common CT volume upstream of the beam. (b) shows the framework for obtaining SPR by dose calculation.
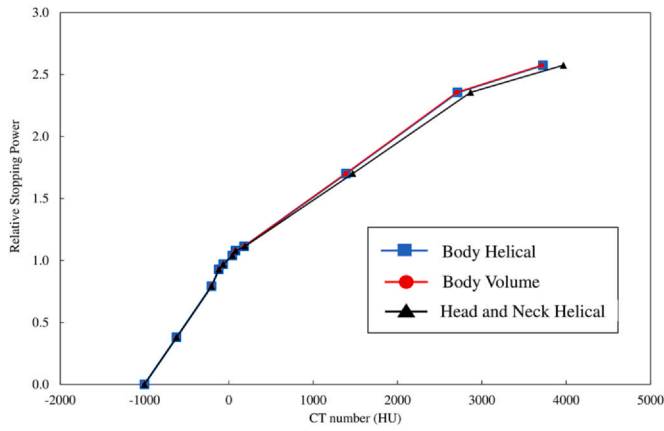
Figure 3. CT-SPR calibration table for each CT protocol obtained by the calibration method based on the polybinary tissue model.

$$SPR_{meas.x} = \frac{Range_{meas,air} - Range_{mes,x}}{Range_{meas,air} - Range_{mes,water}} \quad (4)$$

where $Range_{meas,air}$ is the depth of the maximum dose with air in the container and $Range_{meas,x}$ is the depth of the maximum dose when each material is measured in the container. The difference in range divided by $Range_{meas,water}$, which is the range of the container when it is filled with water, was obtained from the measurement. The difference between the $SPR_{meas,x}$ and $SPR_{register,x}$ for each material x estimated from the CT-SPR calibration table registered in the treatment planning system was calculated using the following equation:

$$Diff_{meas.}(\%) = \frac{SPR_{meas,x} - SPR_{register,x}}{SPR_{register,x}} \times 100 \quad (5)$$

Results

CT-SPR calibration

The relationship between the CT numbers and SPR is shown in a curve in Figure 3. The Body Helical and Head and Neck protocols showed differences in the region of high CT numbers, with a maximum difference of 242.5 HU. The Body Helical and Body Volume curves almost overlapped, with the largest difference in the CT numbers being 15.7 HU.

Verification by dose calculation

The SPR calculated from the dose calculation and the SPR registered in the treatment planning system are shown in Figure 4(a). The difference between 2000 and 1000 HUs was within 1.0%, but at 2000 HUs a difference of about 1.8% and a maximum of about 3.2% was observed. The difference between the SPR from dose calculation and registered SPR and the difference between the SPR for particle energies of 131 and 430 MeV/u that can be derived from the theoretical equation are shown in Figure 4(b). Both results agreed within 0.15% for the SPR of < 2.0 or less and within 0.51% for the SPR of > 2.0.

Verification by measurement

A comparison of the SPR values calculated from the CT numbers of the 5 materials and the maximum dose depth of the beam transmitted through each material with the SPR values calculated from the CT-SPR calibration and the errors are shown in Table 2. Deviation between $SPR_{meas.}$ and $SPR_{register.}$ were within 2.0% for all materials.

Discussion

We reported on the commissioning of CT-SPR calibration at a new start-up facility for carbon-ion radiotherapy. The CT-SPR calibration table was obtained using a method based on the polybinary tissue model, and the commissioning of the CT-SPR calibration was performed. As a result, we concluded that the errors were within the acceptable range for particle therapy and that the CT-SPR calibration table could be used clinically.

We evaluated whether the CT-SPR calibration table registered in the treatment planning system was accurately considered in the dose calculation. In RayStation, the SPR is corrected depending on the energy of the particles, and the effect was confirmed from the present results. It is known that the SPR of a material depends on its energy, as reported by Schneider et al,[8] and the dose calculation results were theoretically provable. This study revealed that it is possible to confirm the registered CT-SPR calibration table from the results of dose calculations. The method used in this study will allow us to compare CT-SPR calibration table using a unified method of dose calculation, regardless of the treatment planning system or CT-SPR calibration method.

It is necessary to pay attention to the treatment outside the CT-SPR calibration table for each treatment planning system. The results shown in Figure 4 indicate that at high CT numbers, a difference of more than 3.0% was identified between the registered table and the dose calculation. This suggested that there is a limit to the accuracy that can be considered in planning. For example, in the RayStation, the CT number below the registered minimum CT number is replaced with a CT number equivalent to the minimum CT number, and the CT number above the maximum CT number is replaced with a constant value equivalent to the maximum CT number. Low CT numbers are not a major clinical problem; however, high CT numbers may be related to metals in the body and should be handled with care. It is recommended that treatment plans use beam angles that do not pass through high HU materials. In cases where the beam must pass through a high CT region, the margin should be adjusted to account for an additional 3% range error.

By dose measurement, we have confirmed the accuracy of estimating the SPR from the CT numbers performed in this commissioning. Yang et al stated that the error introduced by single-energy CT in CT-SPR conversion from soft tissue to bone in standard human tissue can be as high as 4.35%.[26] However, they also reported that the use of dual-energy CT could reduce the error by 0.26%. Schaffner et al. estimated errors due to a stoichiometric method from measurements of soft tissue samples from animals.[27] They stated that if the beam-hardening effect could be ignored, the error would be within 1%. However, because of the actual beam-hardening effect, they estimated a range error of 1.1% for soft tissue and 1.8% for bone tissue, which corresponds to a range error of approximately 1 to 3 mm. Paganetti predicted a variation of approximately 3.5% in CT-SPR conversion by considering a 2% variation in CT values on CT machines and a 1% variation in the change from CT values to SPR.[28] Considering the theoretical error in converting the estimated single-energy CT values to SPRs, in addition to the error introduced by dosimetry, the results of this study are comparable to those previously reported. Therefore, we judged that the obtained CT-SPR calibration table could be used in clinical practice. As an ongoing operation, it will be performed as Daily QA to evaluate the variation of HU value using a solid phantom. We will also reacquire and compare CT-SPR calibration tables for annual QA or for each replacement of a component that may affect the X-ray spectrum to ensure accuracy.

In addition to providing margins for treatment planning to account for errors resulting from the CT-SRP conversion process, RayStation allows us to account for range uncertainty in the robust optimization process. The usefulness of the range uncertainty tool in particle therapy planning on the RayStation was reported by Wagenaar et al.[29] Therefore, at our center, we decided to consider the uncertainty of the CT-SPR conversion process in the treatment planning by setting the range
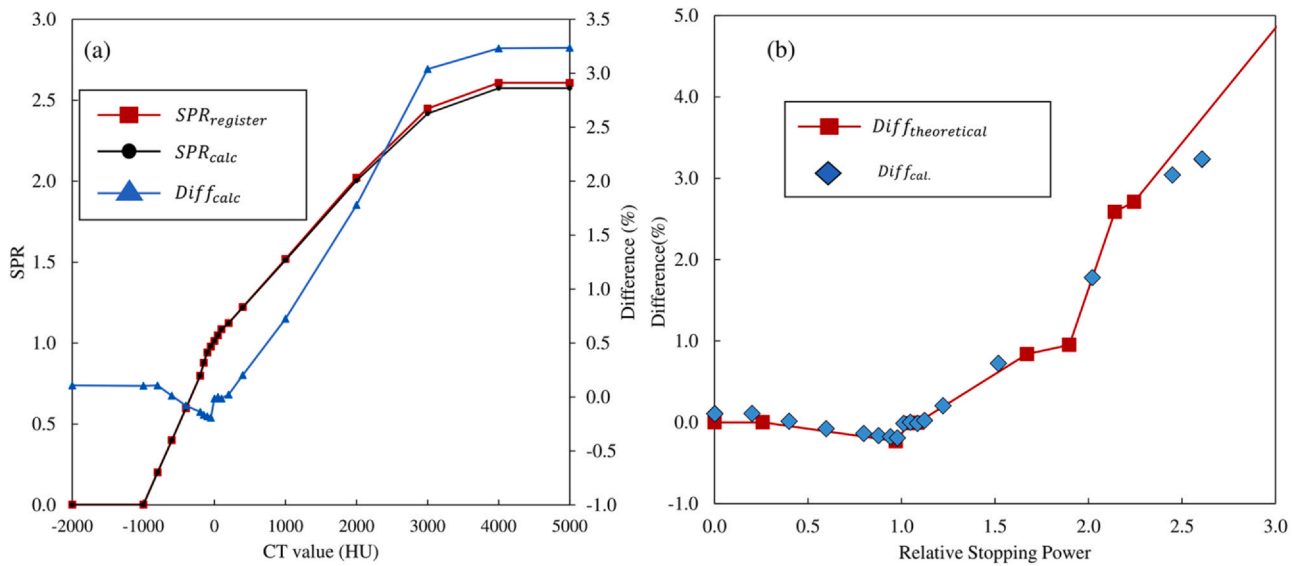
Figure 4. (a) shows the SPR obtained by dose calculation, the SPR registered in the treatment planning system, and the difference between the SPRs. (b) shows the difference between the SPR calculated from the theoretical equation by the difference between the energy of the incident particle 131 MeV/u and 430 MeV/u and the SPR calculated by the dose calculation.

uncertainty tool of approximately 3% in addition to the margin.

Differences were observed in the Body Helical scan and Head and Neck scan protocol data, especially in volumes with high CT numbers. This is an effect of the difference in phantom size. Emma et al has reported that of the several phantoms they verified, they observed large differences in the CT numbers between the large and small phantoms.[3] Similarly, Yagi et al have reported that they observed a difference in the region of high CT numbers in the small-subject head protocol compared with the large-subject body protocol.[30] A similar trend to their report was confirmed in this report. This may be due to the differences in the degree of beam-hardening depending on the phantom size. This effect is greatest in high CT number volumes, that is, mainly the bone volumes in the human body, but may be apparent in the head and neck region because of the dense bone population there. It is important to calibrate by acquiring data under the protocol used in clinical treatment planning, including subject size and artifact reduction algorithms.[31,32]

There is a limitation in this study. In the validation by measurement, we used substitute materials (milk and olive oil) instead of the tissue equivalent materials. Ideally, this study should have been extended to fresh substances such as meat, but we chose to improve the accuracy of the measurements because of the homogeneity of the equivalent substances and limited the substances verified. Similarly, Yagi et al used readily available materials, such as milk and lard.[30] Moskvin et al validated on the calculation of SPRs for inorganic and organic materials and reported comparable results.[33] Therefore, there should be no extreme change in the accuracy between fresh and inorganic materials, and the results of this study are considered acceptable for application to fresh materials. The highest CT value for any material measured in this study was 624 HU for the 40% K_2HPO_4 solution1. The polybinary calibration method reported by Kanematsu et al[9,10] was used to estimate

the CT values for 11 substances from only 4 substances: air, water, 100% ethanol, and a 40% K_2HPO_4 solution. From this, it is presumed that air, water, 100% ethanol, and 40% K_2HPO_4 solutions are important and that if there are no errors in these substances, at a minimum, the other substances are minimally accurate for clinical use. Ideally, however, verification should be conducted for substances exceeding 1000 HU and should be extended to a variety of other substances.

Conclusion

Commissioning of treatment planning CT at a new particle therapy facility was performed. In this process, the accuracy of the CT-SPR calibration table registered in the treatment planning system was checked by dose calculation and measurement to ensure that it is applicable to the treatment. Our results confirm the error of the SPR estimation in the treatment. We were able to determine that the error was within the range that can be expected in general particle therapy and was acceptable for our clinical use.

Author Contributions

Yuya Miyasaka: writing the manuscript, creating treatment plan and data analysis. **Takayuki Kanai:** data analysis, coordination responsibility for the research activity planning and execution and review manuscript. **Hikaru Souda:** data analysis and review manuscript. **Yoshifumi Yamazawa:** data acquisition and review manuscript. **Sung Hyun Lee:** data analysis and review manuscript. **Hongbo Chai:** review data and manuscript review. **Hiraku Sato:** clinical integration, clinical review and review manuscript. **Takeo Iwai:** management and coordination responsibility for the research activity planning and

Table 2

SPRs from the CT-SPR calibration table, SPRs obtained by dosimetry, and the error between the SPRs.

	CT number (HU)	SPR register	SPR meas	Difference (%)
Water	1.56	1.01	1.00	-1.39
100% ethanol	-198.09	0.80	0.82	1.82
40% K_2HPO_4	624.01	1.33	1.31	-1.65
Milk	28.42	1.03	1.03	-0.44
Olive oil	-102.14	0.94	0.94	-0.52

Abbreviations: CT, computed tomography; HU, hounsfiled unit; SPR, stopping power ratio.

execution.

Declaration of Conflicts of Interest

The authors have no conflicts of interest to disclose.

Acknowledgment

References

1. Constantinou C, Harrington JC, DeWerd LA. An electron density calibration phantom for CT-based treatment planning computers. *Med Phys.* 1992;19:325–327.
2. Cozzi L, Fogliata A, Buffa F, Bieri S. Dosimetric impact of computed tomography calibration on a commercial treatment planning system for external radiation therapy. *Radiother Oncol.* 1998;48:335–338.
3. Inness EK, Moutrie V, Charles PH. The dependence of computed tomography number to relative electron density conversion on phantom geometry and its impact on planned dose. *Aust Phys Eng Sci Med.* 2014;37:385–391.
4. Mustafa AA, Jackson DF. The relation between x-ray CT numbers and charged particle stopping powers and its significance for radiotherapy treatment planning. *Phys Med Biol.* 1983;28:169–176.
5. Moyers MF, Sardesai M, Sun S, Miller DW. Ion stopping powers and CT numbers. *Med Dosim.* 2010;35:179–194.
6. Taasti VT, Baumer C, Dahlgren CV, et al. Inter-centre variability of CT-based stopping-power prediction in particle therapy: Survey-based evaluation. *Phys Imaging Radiat Oncol.* 2018;6:25–30.
7. Peters N, Wohlfahrt P, Dahlgren CV, et al. Experimental assessment of inter-centre variation in stopping-power and range prediction in particle therapy. *Radiother Oncol.* 2021;163:7–13.
8. Schneider U, Pedroni E, Anthony L. The calibration of CT Hounsfield units for radiotherapy treatment planning. *Phys Med Biol.* 1996;41(14):111–124.
9. Kanematsu N, Matsufuji N, Kohno R, Minohara S, Kanai T. A CT calibration method based on the polybinary tissue model for radiotherapy treatment planning. *Phys Med Biol.* 2003;48:1053–1064.
10. Kanematsu N, Inaniwa T, Nakao M. Modeling of body tissues for Monte Carlo simulation of radiotherapy treatments planned with conventional x-ray CT systems. *Phys Med Biol.* 2016;61:5037–5050.
11. Peters N, Trier Taasti V, Ackermann B, et al. Consensus guide on CT-based prediction of stopping-power ratio using a Hounsfield look-up table for proton therapy. *Radiother Oncol.* 2023;184:109675.
12. Yang M, Wohlfahrt P, Shen C, Bouchard H. Dual- and multi-energy CT for particle stopping-power estimation: current state, challenges and potential. *Phys Med Biol.* 2023;68.
13. Cui X, Jee K, Hu M, Bao J, Lu H-M. Improvement of proton beam range uncertainty in breast treatment using tissue samples. *Phys Med Biol.* 2022;67.
14. Xie Y, Ainsley C, Yin L, et al. Ex vivo validation of a stoichiometric dual energy CT proton stopping power ratio calibration. *Phys Med Biol.* 2018;63.
15. Iwata Y, Fujimoto T, Matsuba S, et al. Beam commissioning of a superconducting rotating-gantry for carbon-ion radiotherapy. *Nucl Instrum Methods Phys Res Sect A.* 2016;834:71–80.
16. Hara Y, Hara T, Mizushima K, et al. Commissioning of full energy scanning irradiation with carbon-ion beams ranging from 55.6 to 430 MeV/u at the NIRS-HIMAC. *Nucl Instrum Methods Phys Res Sect B.* 2017;406:343–346.
17. Grevillot L, Osorio Moreno J, Letellier V, et al. Clinical implementation and commissioning of the MedAustron Particle Therapy Accelerator for non-isocentric scanned proton beam treatments. *Med Phys.* 2020;47:380–392.
18. Mori S, Sakata Y, Hirai R, et al. Commissioning of a fluoroscopic-based real-time markerless tumor tracking system in a superconducting rotating gantry for carbon-ion pencil beam scanning treatment. *Med Phys.* 2019;46:1561–1574.
19. Mizuno H, Saito O, Tajiri M, et al. Commissioning of a respiratory gating system involving a pressure sensor in carbon-ion scanning radiotherapy. *J Appl Clin Med Phys.* 2019;20:37–42.
20. Hamatani N, Tsubouchi T, Takashina M, Yagi M, Kanai T. Commissioning of carbon-ion radiotherapy for moving targets at the Osaka Heavy-Ion Therapy Center. *Med Phys.* 2022;49:801–812.
21. Kusano Y, Minohara S, Ishii S, et al. Development of the QA/QC-tools for CT number calibration of the treatment planning CT-scanner. *Jpn J Med Phys.* 2006;26:163–172.
22. Kusano Y, Uesaka S, Yajima K, Kumagai M, Mizuno H, Mori S. Positional dependence of the CT number with use of a cone-beam CT scanner for an electron density phantom in particle beam therapy. *Radiol Phys Technol.* 2013;6:241–247.
23. Inaniwa T, Kanematsu N. Effective particle energies for stopping power calculation in radiotherapy treatment planning with protons and helium, carbon, and oxygen ions. *Phys Med Biol.* 2016;61:542–550.
24. Inaniwa T, Kanematsu N. A trichrome beam model for biological dose calculation in scanned carbon-ion radiotherapy treatment planning. *Phys Med Biol.* 2015;60:437–451.
25. RaySearch Laboratories AB, RayStation 10A Reference Manual. 2020.
26. Yang M, Virshup G, Clayton J, Zhu XR, Mohan R, Dong L. Theoretical variance analysis of single- and dual-energy computed tomography methods for calculating proton stopping power ratios of biological tissues. *Phys Med Biol.* 2010;55:1343–1362.
27. Schaffner BP. E. The precision of proton range calculations in proton radiotherapy treatment planning: experimental verification of the relation between CT-HU and proton stopping power. *Phys Med Biol.* 1998;43(13):1579–1592.
28. Paganetti H. Range uncertainties in proton therapy and the role of Monte Carlo simulations. *Phys Med Biol.* 2012;57:99–117.
29. Wagenaar D, Kierkels RGJ, van der Schaaf A, et al. Head and neck IMPT probabilistic dose accumulation: feasibility of a 2 mm setup uncertainty setting. *Radiother Oncol.* 2021;154:45–52.
30. Yagi M, Tsubouchi T, Hamatani N, et al. Commissioning a newly developed treatment planning system, VQA Plan, for fast-raster scanning of carbon-ion beams. *PLoS One.* 2022;17:e0268087.
31. Zhao J, Wang W, Shahnaz K, et al. Dosimetric impact of using a commercial metal artifact reduction tool in carbon ion therapy in patients with hip prostheses. *J Appl Clin Med Phys.* 2021;22:224–234.
32. Miki K, Mori S, Hasegawa A, Naganawa K, Koto M. Single-energy metal artefact reduction with CT for carbon-ion radiation therapy treatment planning. *Br J Radiol.* 2016;89:20150988.
33. Moskvin VP, Pirlepesov F, Yan Y, et al. Accuracy of stopping power ratio calculation and experimental validation of proton range with dual-layer computed tomography. *Acta Oncol.* 2022;61:864–868.